AB

LBL-35295
UC-414
SW 9427

Lawrence Berkeley Laboratory
UNIVERSITY OF CALIFORNIA

Presented at the Tenth Winter Workshop on Nuclear Dynamics,
Snowbird, Utah, January 15–22, 1994, and to be published
in the Proceedings

Hadron Production in S+nucleus Collisions at 200 GeV/nucleon

S. Margetis and The NA35 Collaboration

March 1994

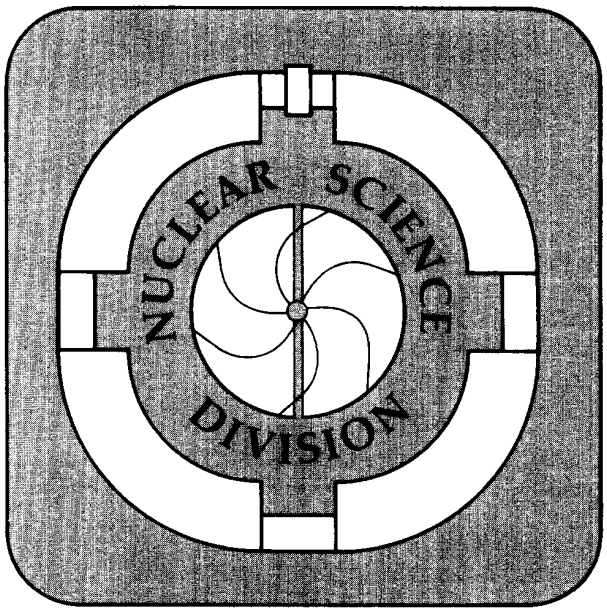

Prepared for the U.S. Department of Energy under Contract Number DE-AC03-76SF00098

LBL-35295
UC-414

Presented at the 10th Winter Workshop on Nuclear Dynamics
Snowbird, Utah, USA
January 15-22, 1994, and to be published in the Proceedings

Hadron Production in S+nucleus Collisions at 200 GeV/nucleon

Spiros Margetis
Lawrence Berkeley Laboratory
University of California, Berkeley, CA 94720

and

The NA35 Collaboration

March 1994

This work was supported by the Director, Office of Energy Research, Division of Nuclear Physics of the Office of High Energy and Nuclear Physics of the U.S. Department of Energy under Contract DE-AC03-76SF00098

Hadron Production in S+nucleus Collisions at 200 GeV/nucleon

S. MARGETIS for the NA35 Collaboration
Lawrence Berkeley Laboratory
Berkeley, CA 94720, USA

ABSTRACT

We present recent results on strange particle production and baryon rapidity distributions from the experiment NA35 at CERN.

1. Introduction

Central collisions between nuclei at relativistic energies form a hot and dense hadronic system over a large volume. Phenomenological models, as well as QCD calculations on the lattice, predict a phase transition in nuclear matter leading to deconfinement, a state of matter in which quarks and gluons are free to move inside the entire volume of the deconfined region. This new state was given the name of Quark Gluon Plasma (QGP). Based on the conjecture that collisions of heavy nuclei at high energies can create the necessary condition of a high energy density thermalized system, a series of experiments were built to search for possible signals of QGP creation.

The NA35 collaboration uses a wide acceptance apparatus at the CERN SPS which detects the majority of charged hadrons ($h^{\pm}$), and neutral strange particles produced in reactions of p, ^{16}O and ^{32}S projectiles at 60 and 200 GeV/nucleon lab momentum on different targets[1,2]. It consists of two major tracking devices which provide the momentum measurement of the charged particles: a 2 m long streamer chamber (SC) which is placed inside a 1.5 T vertex magnet, viewed by three cameras, and a 2.5x1.5x1.0 m^3 Time Projection Chamber (TPC)[3]. The SC covers the backward and the TPC the forward rapidities[4]. A set of calorimeters was used as the basic trigger device of the experiment, to select central (small impact parameter) collisions[2]. In the data presented here, a calorimeter placed in the beam path selects near head-on collisions, i.e. events where only a small amount of energy (mostly spectator nucleon energy) was detected in an angular acceptance of less than 0.3 degrees around the beam axis. The data sample consists of three systems: S+S, S+Ag and S+Au at 200 GeV/c with trigger cross section of 3, 3.2 and 6 % of the total inelastic cross section, respectively.

All the TPC data were computer analysed. In the SC either a computer or an operator performed the pattern recognition task, i.e. to measure the trajectories of

charged particles. No particle identification information was obtained on a track-by-track basis. Charged kaons (K^+, K^-) were identified by their characteristic one and three prong decays in the SC[5] and the TPC[6], as well as V_0 decays (K^0_s, Λ and $\overline{\Lambda}$ particles) by their characteristic decay topology in the SC.

2. Net Baryon Production

The distribution of the initial baryons in the final state can provide valuable information about the reaction dynamics of the colliding system, such as the fraction of the initial energy deposited in the interaction volume as well as the nature of the environment (baryon rich or baryon free). Large degrees of inelasticity, or stopping, are indicated by a large shift in rapidity of the participant nucleons towards midrapidity. The 'lost' or deposited energy is mostly used in particle production, which is discussed below.

In a system like S+S, which has zero net isospin, information about the net distribution of protons (p–$\overline{\text{p}}$) can be extracted using the charge excess technique[7]:

$$\frac{dN_{+,-}}{dy}(\text{AA} \rightarrow \text{p}) = \frac{dN}{dy}(\text{AA} \rightarrow \text{h}^+) - \frac{dN}{dy}(\text{AA} \rightarrow \text{h}^-)$$

This is a good approximation over all rapidities for collisions between isoscalar nuclei. It is also valid for asymmetric systems when the projectile is an isoscalar, if the measurement is performed in the projectile fragmentation region, i.e. forward of midrapidity[1]. The raw signal is corrected for geometrical acceptance asymmetries, effective rapidity shifts in weak decays (e.g. $\Lambda \rightarrow \text{p}\pi^-$), the excess of protons produced in secondary hadron–nucleus interactions, and the observed excess of K^+ over K^- in this experiment.

Figure 1 shows the preliminary net proton and Λ rapidity distributions for S, Ag and Au targets. The net baryon number around midrapidity is large and it increases with the target mass. The total net baryon number (participating baryons) is calculated using the following equation,

$$<\text{B} - \overline{\text{B}}> = 2(\text{p} - \overline{\text{p}}) + 1.6(\Lambda - \overline{\Lambda})$$

with the factor of 2 accounting for the neutrons and the empirical factor 1.6 for the unobserved charged Σ decays[8]. The total net baryon number results are summarized in the first two columns of Table 1.

The extrapolation to 4π in the S+S system was made by reflecting the measured distributions around midrapidity for this symmetric system. In S+Ag the average of the S+S and S+Au distributions was taken, since the mass of Ag is the average of S and Au masses. The quoted errors in the table reflect the systematic uncertainties of this method. The numbers in parenthesis in the first column are the total number of

[1]In this article, the term midrapidity denotes half the beam rapidity and not the *c.m.* rapidity of the system which is slightly different for asymmetric systems

	$<B-\overline{B}>_{4\pi}$	$d(B-\overline{B})/dy\ y=y_{NN}$	$\frac{(\Lambda-\overline{\Lambda})}{(p-\overline{p})}\ 4\pi$	$<h^->$	$<h^->/<B-\overline{B}>$
S+S	52±5 (56)	8.6±1 (0.15)	0.24±0.02	95±5	1.8±0.2
S+Ag	90±10 (93)	15.0±1 (0.16)	0.22±0.04	160±8	1.8±0.2
S+Au	— (110)	22.0±1 (0.20)	—	—	—

Table 1: Net baryon, negative hadron multiplicities and rapidity densities in S+S, Ag, Au collisions (see text).

participants predicted by a clean-cut geometry model. The numbers in parenthesis in the second column are the net baryon density around midrapidity per participant nucleon. We observe that it increases with increasing target mass, indicating an increasing stopping for the heavier systems. This can be seen, in a qualitative manner in fig. 1a where for the heavier targets a change of the slope of the distribution forward of midrapidity brings more protons in the region around midrapidity depleting at the same time the region close to beam rapidity. In S+Ag, the large number of target protons results in the high peak at small rapidities.

In order to be more quantitative the mean rapidity shift ($<\Delta y>$) of the participating nucleons in the reaction has been calculated. It was found to be $<\Delta y>= 1.78 \pm 0.09$ for the system S+Au[9] and $<\Delta y>= 1.58 \pm 0.15$ in S+S[7]. This can be compared to $<\Delta y>\approx 1$ in nucleon-nucleon collisions. A relatively large amount of stopping is observed especially for the S+Au system.

The two last columns of Table 1 give information about the negative hadron (mostly pions) production in these systems. Notice the same number of produced negative hadrons per net baryon for the S+S and S+Ag systems.

3. Strange particle production

New results on strangeness production in the S+Ag system exhibit an enhancement relative to nucleon–nucleon collisions, which was previously observed in ref. [10] for central S+S collisions. In order to make comparisons, the measured yields are extrapolated over the full phase space. In the case of S+Ag the measurements cover the rapidity region up to midrapidity with a low p_T cut of 0.5 GeV/c. In order to be able to measure S+Au interactions forward of midrapidity, an additional magnet was placed upstream of the SC. The extrapolation in p_T was done by first fitting the transverse mass distributions m_T with an exponential function of the form:

$$\frac{1}{m_T}\frac{dN}{dm_T} = A \cdot e^{-m_T/T}$$

and then calculating the yield in 4π by integrating the fitted function. The effective temperature parameter T was found to be almost the same for every strange particle species we measured, around 200 MeV.

The extrapolation in rapidity was based upon the observation that the strange particle production in the forward hemisphere in systems with the same projectile nucleus is roughly independent of the target. This can be seen in fig. 2a,b,c where preliminary rapidity distributions for Λ, K^0_s and $\overline{\Lambda}$ are shown. We observe that above rapidity 3 the yield of Λ, $\overline{\Lambda}$ and K^0_s is similar in the S+S and S+Au systems, therefore, for the S+Ag system, the average of the above systems was taken. The curves in the Λ and K^0_s distributions show p+S data multiplied by a factor of 29. It was found that multiplying the negative hadron distributions in p+S by this factor one could reproduce those in S+Ag reactions. This comparison is made model independent because models do not satisfactorily describe strangeness production at the fundamental nucleon–nucleon level[12].

Figures 3a,b show the preliminary K^+ and K^- rapidity distributions for the S+S and S+Ag system. The p+S data are also shown scaled up by the same factor 29 as before. We observe that the S+Ag data are systematically higher than the scaled p+S data and that the difference reaches its maximum for the Λ and K^+ particles. This is qualitatively expected since the quark content of a baryon rich environment, like the target fragmentation region of the heavy Ag target, favors interactions of an 'associated production' type, i.e. p+X $\rightarrow$ $K^+\Lambda$+X. This is further

	$<h^->$	$<\Lambda+\Sigma^0>$	$<\overline{\Lambda}+\overline{\Sigma}^0>$	$<K^0_s>$	$<K^+>$	$<K^->$
S+Ag	160±8	13.0±0.7	2.4±0.4	13.2±1.1	17.4±1.0	9.6±1.0
50∗NN	—	4.8±0.5	0.7±0.2	10.0±1.0	12.0±3.0	8.5±2.5
p+S	5.7±0.2	0.28±0.02	0.043±0.003	0.38±0.04	—	—
S+S	95±5	8.2±0.9	1.5±0.4	10.6±2.0	12.5±0.4	6.9±0.4
30∗NN	—	2.9±0.3	0.4±0.1	6.0±0.6	7.2±1.9	5.1±1.6

Table 2: Mean total particle multiplicities in p+S, S+Ag and S+S collisions.

supported by fig. 1b which shows that these net Λs are concentrated around the target fragmentation region of the S+Ag system. Also, the third column of Table 1 shows that the net number of produced Λs per participant nucleon is the same in S+S and S+Ag. This scaling might indicate a relationship between these two particles. It might also explain why the extra particles are appearing in the same rapidity region where the participating nucleons are finally recorded.

How close does the excess of Λ and K^+ particles, as expressed by the distribution of the difference of $\Lambda - \overline{\Lambda}$ and $K^+ - K^-$, follow the distribution of net protons (p $-\overline{p}$) in rapidity? Figure 3c shows the resulting distribution for the $K^+ - K^-$ for the systems S+S and S+Ag. This should be compared to fig. 1a and 1b. We observe that not only do the distributions of net Λ and K^+ closely follow the distribution of the net protons in the final state, but also the abundance of these extra Λ and K^+s are similar. This is a further indication that these extra particles might be produced in

pairs. The above considerations support the idea that most of the enhancement of the Λ and K^+ particles can be attributed to processes similar to associated production. Of course, the exact mechanisms involved cannot be deduced by these experimental observations.

The degree to which flavor symmetry is achieved at the quark level in the final state is usually characterized by the *strangeness suppression* factor λ_s,

$$\lambda_s = \frac{<s+\bar{s}>}{0.5 \cdot (<u+\bar{u}> + <d+\bar{d}>)}.$$

The quantity λ_s can be calculated according to ref. [14] from the numbers in Table 2. We found that λ_s is half as strong in the S+S and S+Ag systems as compared to nucleon–nucleon[13] and nucleon–nucleus[14] systems.

Phenomenological, as well as microscopic string models, have great difficulties in consistently reproducing the observed enhancement in the two systems we have studied thus far. New mechanisms at the parton level are needed, for example, color rope (RQMD[15]) or double string formation (VENUS[16]). For a more detailed comparison with models, see ref. [11].

4. Summary

The following remarks summarize the above discussion:

- NA35 data on baryon distributions in S+Au collisions show high degrees of stopping, manifested in the large mean rapidity shift of the participant protons.
- We observe an increasing mean rapidity shift of the participant protons with increasing target mass.
- The region around midrapidity appears to be baryon rich for all systems.
- New data on strange particle production in S+Ag show a strangeness enhancement relative to nucleon–nucleon and nucleon–nucleus collisions.
- It appears that most of the excess of Λ over $\overline{\Lambda}$, and K^+ over K^-, can be explained by an 'associate production'–like process.

5. ACKNOWLEDGMENTS

This work was supported in part by the Director, Office of Energy Research, Division of Nuclear Physics of the Office of High Energy and Nuclear Physics of the U.S. Department of Energy under constract DE-AC03-76SF00098.

6. References

[1] A. Sandoval *et al.*; NA35 collaboration, Nucl.Phys. A461 (1987) 465c
[2] S. Margetis; Ph.D thesis, GSI–91-04
[3] P. Jacobs *et al.*; NA35 collaboration, LBL–33810

[4] D. Röhrich *et al.*, NA35 collaboration, IKF-HENPG/93-8 and *Proc. of Quark Matter 93*, Nucl.Phys. A566 (1994) 35c
[5] M. Kowalski *et al.*; NA35 collaboration, Nucl. Phys. A544 (1992) 609c
[6] S. Margetis; work in progress.
[7] J. Bächler *et al.*; NA35 collaboration, to appear Phys. Rev. Lett., February (1994)
[8] A.K. Wróblewski; Acta Phys. Pol. B16 (1985) 379
[9] J.T. Mitchell *et al.*; NA35 collaboration, *Proc. of Quark Matter 93*, Nucl.Phys. A566 (1994) 415c and LBL-34727
[10] A. Bamberger *et al.*; NA35 collaboration, Z. Phys. C43 (1989) 25, J. Bartke *et al.*; NA35 collaboration, Z. Phys. C48 (1990) 191
[11] M. Gaździcki *et al.*; NA35 collaboration, *Proc. of Quark Matter 93*, Nucl.Phys. A566 (1994) 503c Also paper in preparation.
[12] I. Sakrejda, proceedings of this workshop.
[13] M. Gaździcki and O. Hansen; Nucl. Phys. A528 (1991) 754
[14] H. Bialkowska *et al.*; Z. Phys. C55 (1992) 491
[15] H. Sorge *et al.*; Phys. Lett. B289 (1992) 6
[16] K. Werner and J. Aichelin, Phys. Lett. B308 (1993) 372

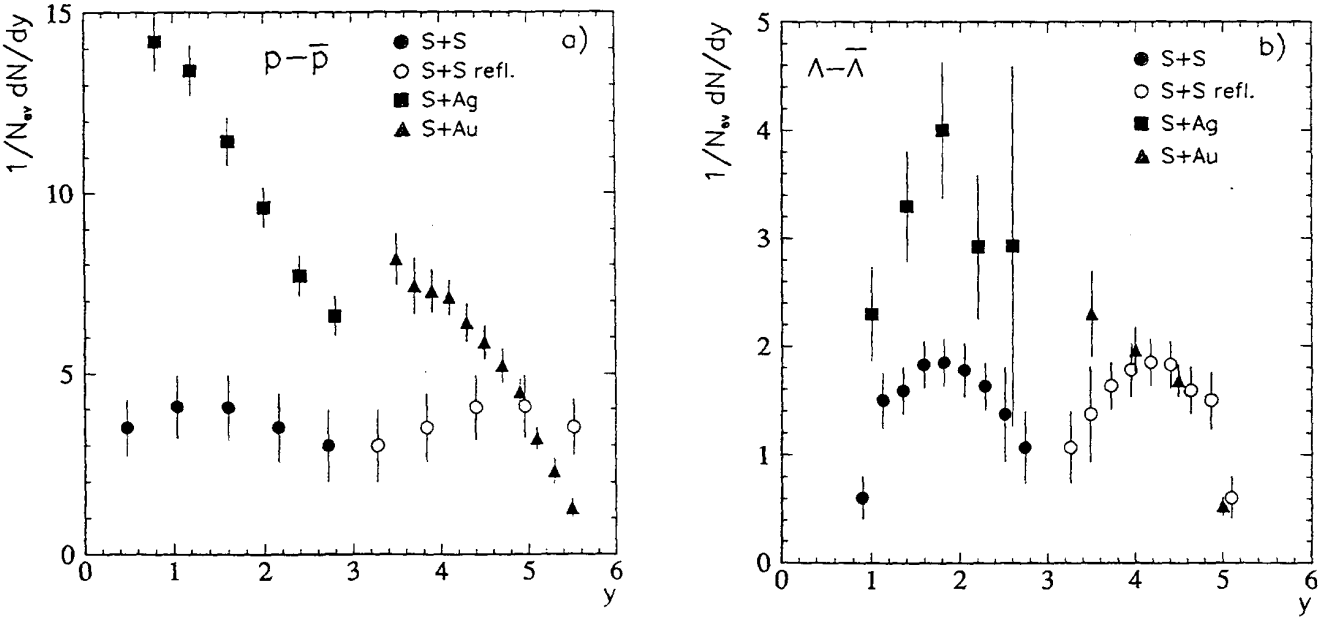

Fig. 1: Rapidity distributions of, a), net protons and, b), net Λ, in S+nucleus collisions.

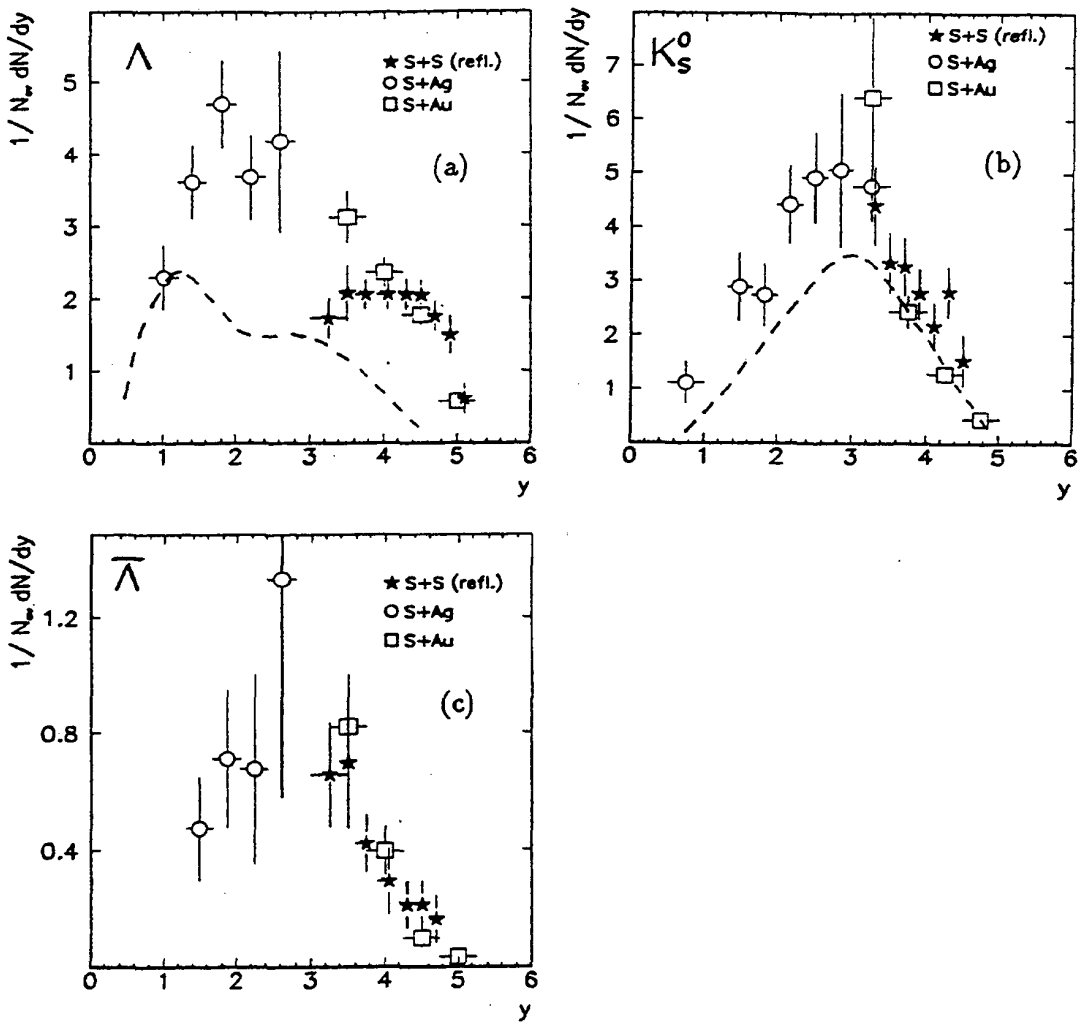

Fig. 2: Rapidity distributions of Λ, K^0_s and $\overline{\Lambda}$ particles in S+nucleus collisions. The dashed curves represent p+S results scaled up by a factor of 29 (see text).

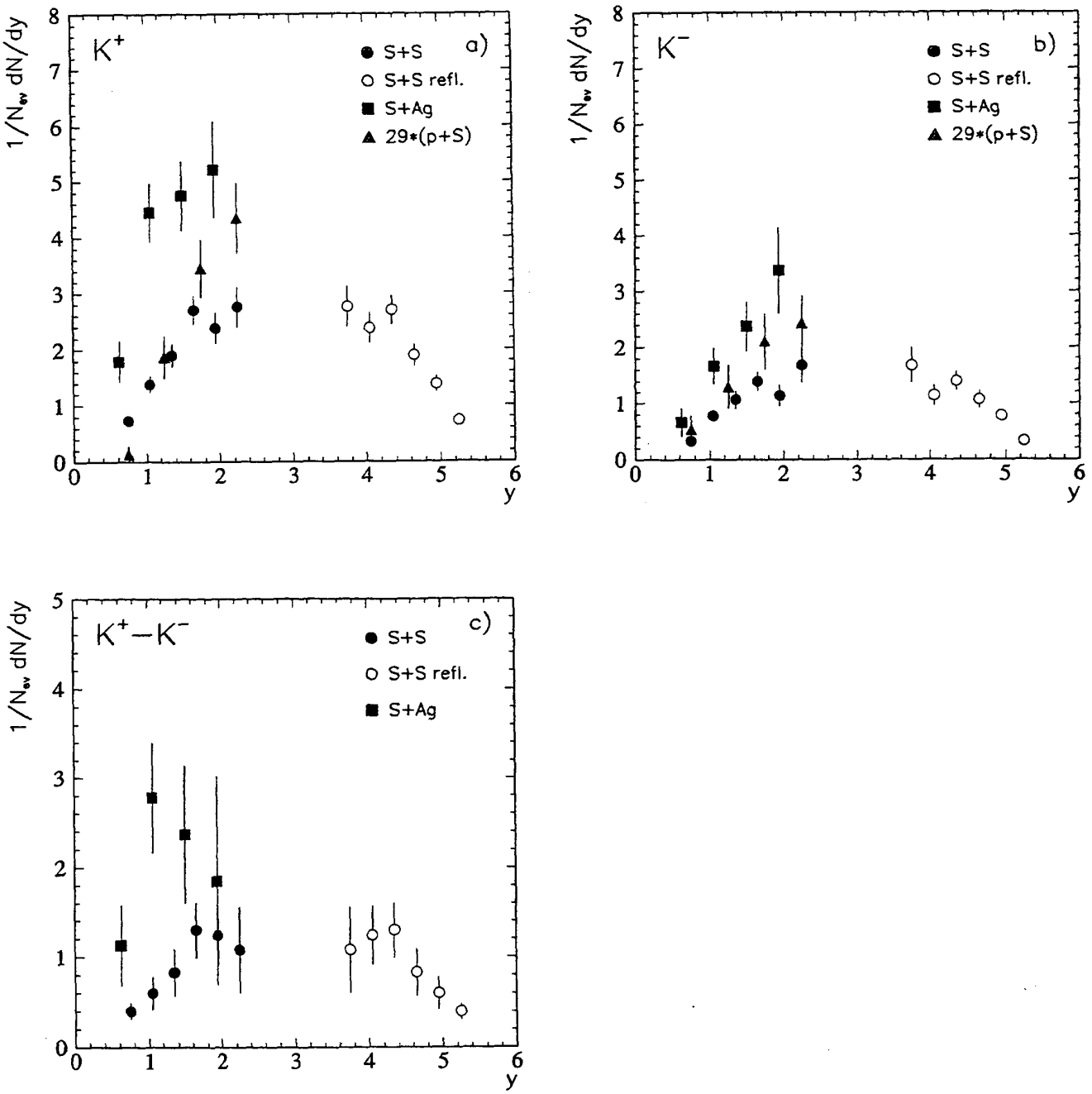

Fig. 3: Rapidity distributions of, a), K^+, b), K^- and, c), net charged kaons in S+nucleus collisions. The p+S results scaled up by a factor of 29 are also shown for comparison.